Emissions and Dynamic Stability Improvements in Premixed CH₄/NH₃ **Swirling Flames with Nanosecond Pulsed Discharges**

Santosh J. Shanbhogue¹, Raphael J. Dijoud², Colin A. Pavan³, and Sankarsh Rao²

Massachusetts Institute of Technology, Cambridge, MA, 02139, USA

Felipe Gomez del Campo⁴

Specter Aerospace, 6 Fifth St, Peabody MA, USA

Carmen Guerra-Garcia⁵ and Ahmed F. Ghoniem⁶ Massachusetts Institute of Technology, Cambridge, MA, 02139, USA

In this paper we explore the effects of nanosecond repetitively pulsed discharges (NRPD) on combustion instabilities and NO_x emissions of CH₄/NH₃ flames, in a swirl-stabilized, 6 kW combustor. The combustor has a large dump plane ratio resulting in a turbulent flame with a single compact macrostructure across all operating conditions. Discharges are setup with a central pin-to-cylindrical-wall type electrode configuration with a discharge gap of 4.55 mm at the dump plane. For pure methane, instabilities occur at various frequencies and amplitudes, up to 1000 Pa. NPRD actuation was successful in suppressing instabilities across all conditions, with best reduction being as much as 23 dB. The discharge voltages ranged from 6-9 kV at a pulse rate of 9 kHz, equivalent to 5-12 mJ/pulse energies and plasma powers less than 99W. For pure CH4 flames, the NRPD actuation increased NO_x emissions, but for high NH₃/CH₄ blends, the NRPD actuation reduced NO_x emissions.

I. Introduction

The quest to decarbonize transportation and power generation has led to an interest in hydrogen carriers such as ammonia and other sustainably produced fuels as replacements for fossil fuels. Regardless of which fuel is adopted in the future, an outstanding challenge will be the need to reduce NO and NO₂ – collectively referred to as NO_x emissions - produced during the combustion of these fuels. Regulations on these emissions are getting only more stringent with time. For aircraft, the International Civil Aviation Organization's (ICAO) CAEP/8 standards mandates NO_x emissions to be within 20-100 g/kN depending on the engine pressure ratio [1]; for ships, the International Maritime Organization (IMO) standards restrict NO_x to 1.96-3.4 g/kWh depending on the engine rpm; and for passenger diesel engines, the Euro VI norms require NO_x emissions less than 0.4 g/kWh as measured on a WHTC driving cycle. For power generating units, NO_x emissions limits are set by local authorities and vary by jurisdiction and fuel type, but the most

¹ Research Scientist, Mechanical Engineering, AIAA Member, santosh1@mit.edu

² Graduate Research Assistant, Aeronautics and Astronautics, AIAA Student Member

³ Post-Doctoral Associate, Aeronautics and Astronautics, AIAA Member

⁴ Chief Executive Officer, AIAA Member

⁵ Draper Career Development Assistant Professor, Aeronautics and Astronautics, AIAA Senior Member

⁶ Ronald C. Crane ('72) Professor, Department of Mechanical Engineering, AIAA Associate Fellow

stringent limits in the US require NO_x to be much less than 0.1 g/kWh. The strictest of these limits equates to nearly 2 ppm when measured on a volumetric and dry basis at 15% O₂.

Measurements of select oxides of nitrogen - NO, NO₂ and N₂O - from combustion of ammonia by itself or blending with hydrogen or methane have been the focus of several recent studies aiming to explore effects of inlet temperature [2], pressure [3, 4], residence time [5], inlet swirl [6], fuel staging [7] and mixture ratio [8] on the emissions. A troubling conclusion from these papers is that compared to a methane/air flame which has maximum NO_x emissions around 100 ppm under stoichiometric conditions; for ammonia/air flames, they can easily exceed 1000 ppm. Secondly, unlike methane air flames where the NO_x emissions peak near stoichiometry, for ammonia blended fuels, NO_x emissions can peak at leaner equivalence ratios, with values beyond 25,000 ppm. NO_x emissions from NH₃/air flames, originating from the fuel, have a non-monotonic dependence on mixture composition (if blended with another fuel) and equivalence ratios.

These emissions from ammonia blended fuels being orders of magnitude higher than those emitted from current combustion systems, will necessitate costly and intensive post-combustion treatment of the flue gases for all end-uses. For aviation, this is particularly troubling as such aftertreatment systems, if at all feasible, will only add weight and volume to aircraft and will interfere with the design of engine turbines, as common catalytic aftertreatment channel the flow through honeycomb-like structures that raise the back pressure, reducing engine thrust levels. Alternatively, one needs methods like either fuel staging [9, 10, 11] with long residence times or novel concepts like nanosecond pulsed discharges [12] to reduce emissions in-situ.

Non-thermal plasmas, mostly using corona reactors, have been shown to reduce NO_x in the tailpipes of diesel engines when coupled with a catalyst [13], but it is yet to be seen if this can be done without a catalyst and in-situ by modifying the combustion process. A further advantage of nanosecond pulsed plasmas is that that they have already been shown to improve a number of other properties desired in combustion systems such as lowering ignition delay and improving flame stability, propagation [14] and dynamics [15, 16, 17] and in most cases with comparatively very low amounts of input power [18, 19] compared to combustor power. Whether nanosecond pulsed plasmas can reduce emissions for all fuels and at what conditions is still unresolved, because studies are done on different combustors and burners with varying electrode designs and at different points within the combustor. As such, studies on CH₄/air flames show that plasmas increase NO_x emissions [20], whereas studies on NH₃/air flames or their blends with methane and hydrogen are reporting that plasmas decrease emissions [12, 21, 22].

Our main interest in this paper is in examining possible ways plasmas can improve characteristics of CH_4/NH_3 flames. Towards this end, we study its effects on the flame macrostructure, instability spectra, and NO_x emissions. We begin by describing the experimental setup and characteristics of the nanosecond repetitively pulsed discharge system next.

II. Experimental Setup

A. Combustor and Emissions Measurement Setup

Experiments were conducted in an atmospheric pressure, non-preheated 6 kW combustor which is nearly 4 m long. A schematic of the combustor is shown in Figure 1. The overall length of the combustor, the pressure sensors and the flowmeters used for metering air and fuel are similar to the combustor described in our previous work [23]. The main difference between our prior work and this study is the swirler, electrode assembly, and the ensuing diameter of the exit nozzle, downstream of which the flame is anchored. In this combustor the fuel/air mixture exits the swirler into the combustion chamber via a 9.1 mm diameter nozzle with a rod electrode with a pointed tip in the center. This causes the plasma to spark from the center of the electrode to the cylindrical wall 4.55 mm away. The exit velocity is nearly 30 m/s and the Reynolds number close to 20,000. These numbers change slightly depending on the mixture composition and equivalence ratio. In all the tests, the air flow rate was kept constant and the fuel flow rate varied to change the equivalence ratio. Pressure sensors are mounted at various locations throughout the combustor, but the spectra reported in this paper correspond to measurements made 1.33 m downstream of the exit nozzle.

Emissions were measured with an AMETEK Lancom 4 flue gas analyzer. This instrument can measure NO from 0-5000 ppm, NO₂ from 0-1000 ppm, O₂ from 0-30%, in addition to CO, CO₂, SO₂ along with the flue gas temperature. All measurements were corrected to a dry, 15% oxygen level. The flue gas probe was mounted 2.64 m downstream

of the nozzle at which point the flue gas temperature reduced to less than 350 K. An important question is whether the measurements at this location downstream of the flame are representative of the NO_x measurements close to the flame. Wang et al. [5] have studied the effect of sampling gases at different locations downstream of the flame and conclude that the sampling location does not significantly affect NO_x measurements. This finding is particularly advantageous as it reduces the need to insert an intricately designed, cooled-probe at high temperature locations close to the flame.

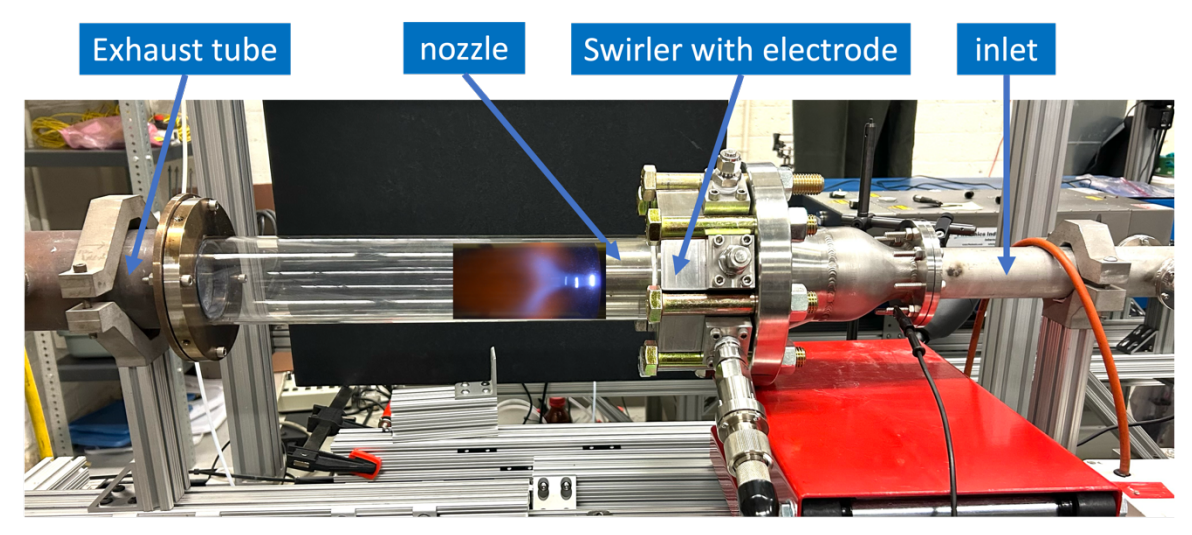


Figure 1: Schematic of the combustor, with an overlaid photograph of flame macrostructure when actuated on by NRPD.

B. Plasma Source and Quantification of the NRP Discharges

Nanosecond pulsed discharges were generated using a TPS transient pulse generator (SSPG-20X-HP1) powered by an AMETEK Sorensen XG 600-2.8 DC power supply. Typical FWHM pulse widths are about 12 ns in duration with a frequency of 9 kHz. Peak voltage, at the measurement location, is 6-9 kV and the energy deposited in the discharge per pulse is 5-12 mJ.

The discharges were characterized using electrical waveforms by the per-pulse energy deposition, as was done in our previous studies[23, 24]. Deployment of other diagnostics, like optical measurements, is not complicated by the swirling, non-localized nature of the pin-to-cylinder discharge. The deposited energy is calculated from time-resolved current and voltage measurements. The combustor geometry restricted direct access to the high-voltage electrode, so electrical measurements were performed at the midpoint of the coaxial cable connecting the high-voltage pulser and the discharge gap. The setup consisted of two identical 5 m coaxial cables connecting the power source and the load, whose shielding was joined together with a small shunt resistance of 0.1Ω . The current is directly measured in the shunt. The corresponding voltage at that location was calculated by multiplying this current by the known cable impedance (50 Ω), while also accounting for the pulse propagation direction (whether it is the forward or reverse wave). The per-pulse energy deposition at the load was then calculated by integrating in time the product of the current and voltage, including the incident pulse and its first reflection, considering power from the source to the load and power reflected back. Further details are provided in our previous work [24]. Minesi et al. [25] employed a similar method to the one described above, referred to as their "remote configuration". The electrical measurements were recorded by a Teledyne Lecroy Waverunner 9254 oscilloscope operating at a sampling frequency of 10 GHz for 1 µs with a bandwidth resolution of 500 MHz, sufficient to capture and resolve the dominant frequencies of the pulse. For the 9 kHz discharge, 4000 pulses were collected. The current shunt probe output was read through a Mini-Circuits HAT-10+ 10 dB attenuator with a 2 GHz bandwidth and a 50 Ω impedance.

Figure 2 and Figure 3 shows respectively, an example of the electrical waveforms measured by this technique and the statistical distribution of per-pulse energies as a function of the peak pulse voltage. The per-pulse energy increases quadratically with voltage, as expected. The variation of the per-pulse energy, at a given voltage, remains within 1 mJ for the majority of the cases studied.

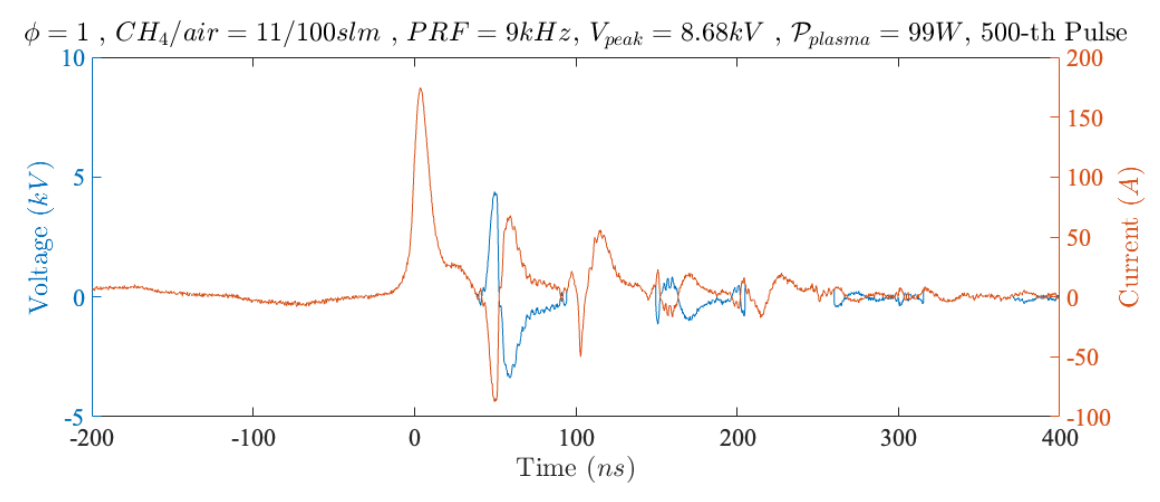


Figure 2: Measurements of voltage (blue, left-axis) and current (orange, right-axis) during a single nanosecond pulse, measured at the shunt resistor.

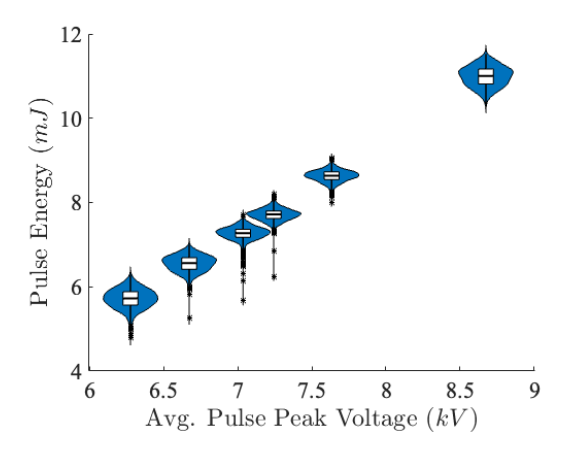


Figure 3: Distribution of the energy deposited per pulse as a function of peak pulse voltage for a stoichiometric CH₄/air flame.

III. Results

We present a preliminary characterization the flame for different equivalence ratios and methane/ammonia blends in §III.A. Next, we report the thermoacoustic characteristics of these mixtures in §III.B and emissions in §III.C. All results are described with and without the nanosecond repetitively pulsed discharges (NRPD) present.

A. Flame Macrostructure Characterization

Chemiluminescence images of pure-methane flames at various equivalence ratios (ϕ) from stoichiometry to 0.6 are shown in Figure 4. Without plasma, at equivalence ratios from 1.0 to 0.7, the flame appears as a vertical band, lifted off from the nozzle, although a closer examination of the image reveals a faint connection to the rim of the nozzle. As the equivalence ratio decreases from stoichiometry, the intensity of the flame decreases, consistent with the decreasing heat-release rate. However, the shape of the flame, or its macrostructure, is nearly identical between $1.0 \le \phi \le 0.7$. At $\phi = 0.6$, the flame appears different as compared to those at higher equivalence ratios. There is no longer a strong vertical band of intense chemiluminescence, rather, the flame appears to be distributed axially.

When the NRPD is turned on at 9 kHz, for all equivalence ratios, the flame shape is completely different. We now see a strong chemiluminescence signal starting from the electrode tip, causing the flame shape to resemble the letter

Y. The plasma at these conditions is clearly successful in modifying the flame macrostructure. Without plasma, the flame blows off somewhere between 0.6 and 0.55. In this setup, so far, the plasma was unsuccessful in extending the blowoff limit as reported in other studies [20].

Equivalence Ratio	Flame image without Plasma	Flame image with Plasma
1.0		
0.9		
0.8		
0.7		
0.6		

Figure 4: Flame macrostructures for CH₄/air flames at various equivalence ratios with and without plasma. The flow direction is from right to left. All experiments with plasma have average pulse energies of 8.64 mJ/pulse.

Flame images for two representative methane/ammonia blends are shown in Figure 5. The highest ammonia fraction for which we could obtain a stable flame was 80% ammonia in the blend. Beyond this, the flame would not anchor at a flow velocity of 30 m/s. The macrostructure of the flame is different when compared to methane/air flames at the same equivalence ratio. This macrostructure resembles that of the methane/air flame at $\phi = 0.6$. However, when mild amounts of ammonia added to the methane/ammonia blend, the macrostructure is unchanged compared to pure methane flames. These compact flames are different from our previous work [23, 26] and other studies in literature [5, 27, 28] that report a variety of macrostructures as the equivalence ratio is decreased from stoichiometry towards the lean limit, especially for ammonia flames and CH₄/NH₃ flames. In particular, close to the lean blowoff limit, many studies report long columnar flames.

Equivalence Ratio	90% CH ₄ /10% NH ₃	20% CH ₄ /80% NH ₃
1.0		
0.9		

Figure 5: Select methane/ammonia flame images for 10% ammonia and 80% ammonia in the blend, without plasma.

B. Dynamic Stability Characteristics

The pressure spectra at different equivalence ratios for a methane/air flame are shown in Figure 6 with and without NRPD. Without the discharges, the combustor exhibited combustion oscillations with strong peaks at all equivalence ratios spanning $1.0 \le \phi \le 0.7$. At stoichiometric conditions, the dominant mode of oscillations was 160 Hz. At $\phi = 0.9$ and 0.8, the strongest peaks are at 230 Hz with smaller peaks in the 160-170 Hz range, and at $\phi = 0.7$ we observe the highest amplitude oscillations of nearly 400 Pa at 160 Hz. Not shown are the spectra for $\phi = 0.6$, because there were no strong peaks and the highest amplitudes at all frequencies were well below 40 Hz.

When the discharge is activated at 9 kHz, we see that in all cases there is total suppression of the instability at all frequencies. This is best quantified by the overall sound pressure levels in decibels or $20log \frac{p_{rms}}{p_{ref}}$, with the reference pressure being 20 μ Pa. The highest SPL in the Figure 6 is 146.22 dB for ϕ = 0.7. The plasma reduces this to 122.98 dB, or a reduction of 23.44 dB. In other cases, for stoichiometric conditions as shown in Figure 7, we see larger amplitudes with a peak of 1000 Pa and with an rms value of nearly 625 Pa. This corresponds to 149.88 dB without plasma and 124.32 dB with plasma, or a reduction of 25.56 dB. For the data in Figure 6, the per pulse energy is 8.64 mJ/pulse corresponding to the ratio of the plasma power to combustor power being slightly more than 1%. These do not correspond to the absolute minimum plasma powers required to suppress the instability, and the objective of this data set was to illustrate one representative plasma operating condition that works across the broadest range of equivalence ratio and instability frequencies.

It is of great interest to note how this ratio of plasma power to combustor power scales with the combustor size/power, to assess how these can be implemented in practical systems that are 100-1000 MW in rated capacity (for e.g., those used in power generation and aviation). The results by Dharmaputra et al. [19] are most promising in this regard. They show that even with similar or even slightly lower plasma powers (as low as 1.1W), they were able to reduce combustion instability amplitudes in a 73 kW sequential combustor. The results from their studies and the present work indicate that the plasma needn't actuate the whole flame, but deposit energy in certain receptive regions to achieve good instability suppression. This implies that the plasma energy needed to actuate the flame doesn't necessarily have to scale linearly with combustor power. Further work is needed to understand this important scaling parameter.

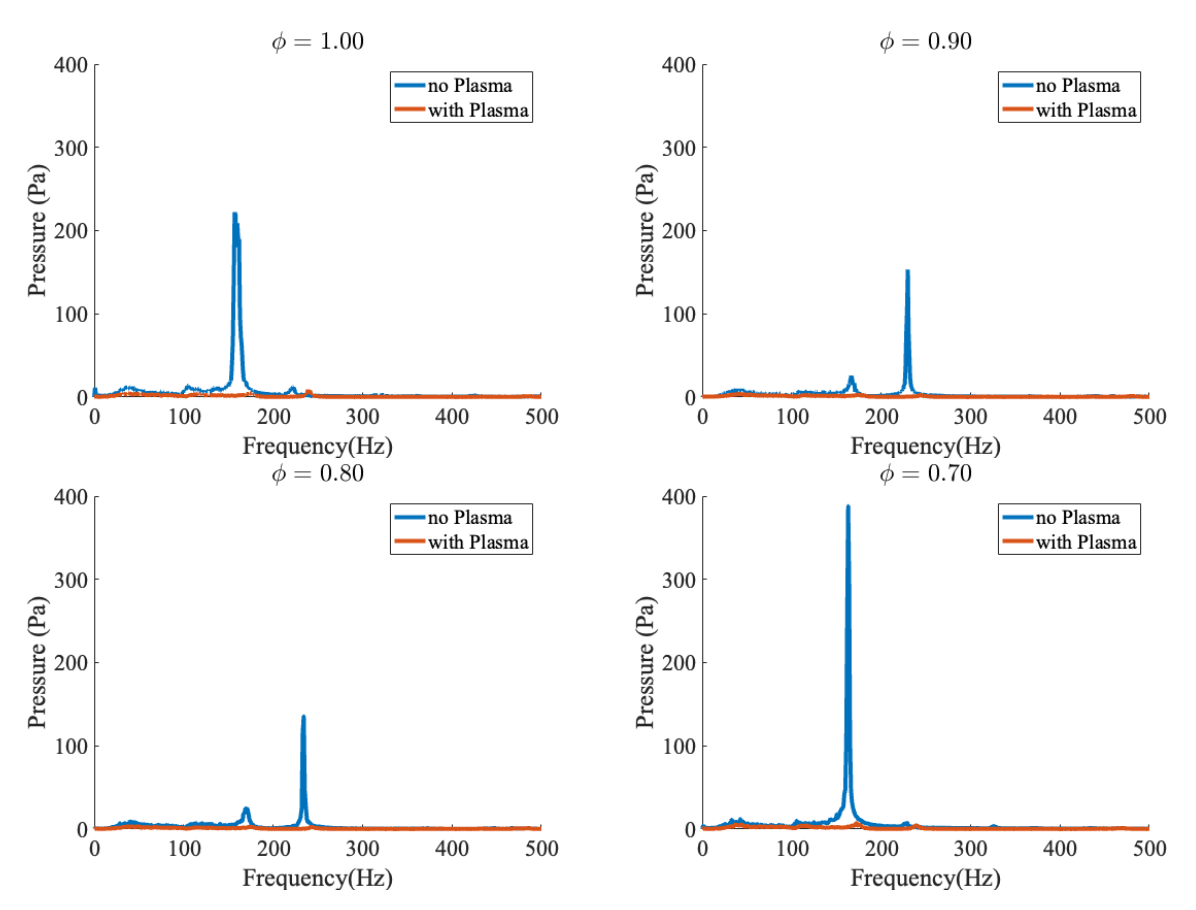


Figure 6: Pressure spectra for CH₄/air flames at different equivalence ratios, with and without plasma. All experiments with plasma have average pulse energies of 8.64 mJ/pulse.

C. Plasma Energy and Instability Reduction

Figure 7 shows the actuation authority of the plasma in terms of reduction of the pressure instability, for different plasma power levels. For all cases, the plasma is activated at t=0, and the recording of electrical measurements is stopped after 1000 pulses, at t=111 ms after the pulsing starts, because of the limited data buffer of the oscilloscope. However, the pulsing continues even after that time although no electrical measurements are taken. We first note that the energy deposited per pulse fluctuates with the pressure oscillations, especially at low plasma actuation energies. This is consistent with the 'backward problem', or the influence of combustion on the plasma development, reported in our prior work [24, 29]. The instability is almost suppressed for plasma power greater than 70W, which is less than 1% of the flame power. For lower plasma power, the instability is only partially reduced. We can also note that the phase of the pressure oscillation sometimes "jumps" discontinuously when the plasma is turned on – this is an artifact of the data acquisition process where the acquisition is stopped and restarted after a few microseconds when the plasma is triggered on.

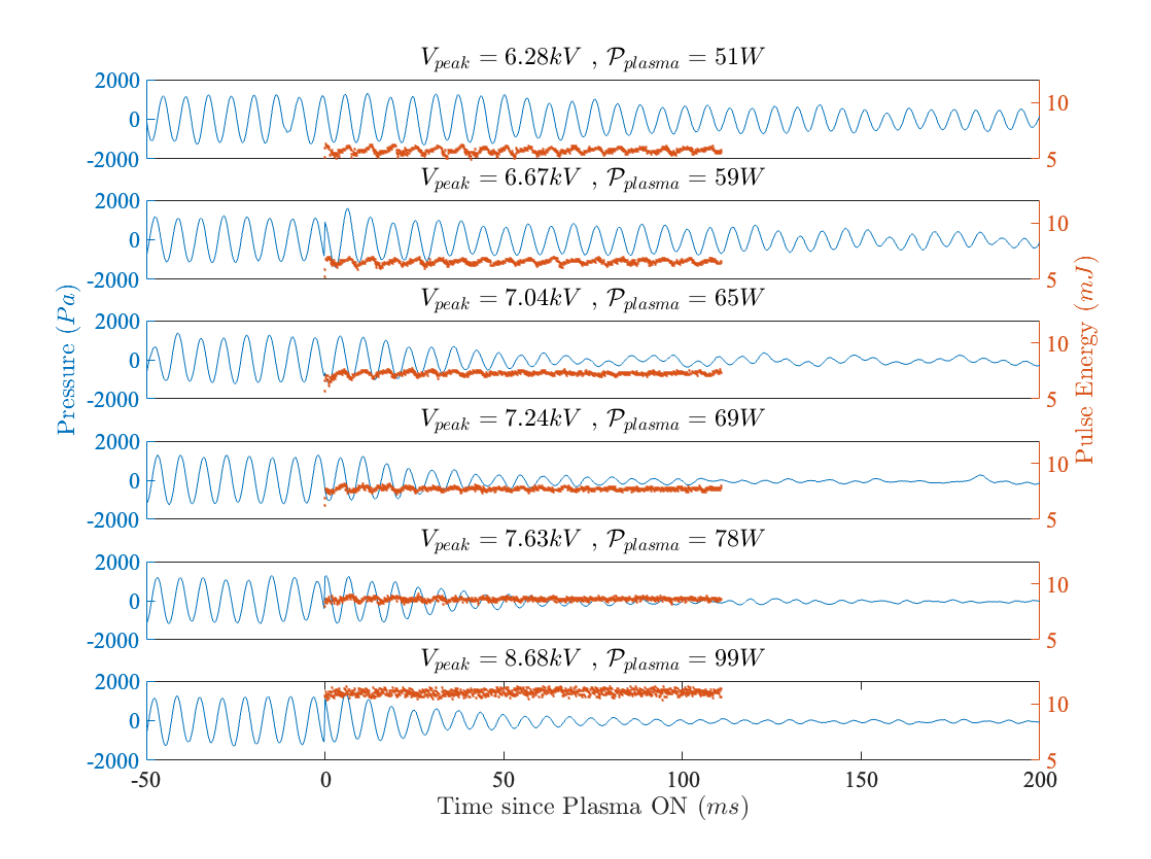


Figure 7: Amplitude of the pressure oscillations (blue) and per-pulse energy deposited by the plasma (orange) for different plasma power, from low power (top) to high power (bottom). All measurements were conducted for a stoichiometric CH4/air flame.

D. NO_x Emissions

NO_x emissions in this combustor for different conditions are plotted in Figure 8. Figure 8 (left) shows the baseline emissions, for methane/air flames at various equivalence ratios. For comparison, we have also included results from two flamelet models along with the measurements. These two models represent an unstrained flame and a flame at the extinction strain rate. These were computed using Cantera and CHEMKIN respectively using the GRI3.0 mechanism. Although the GRI3.0 is a dated kinetic model, and despite higher fidelity and more comprehensive models existing for C1 compounds such as NUIG1.2/1.3 [30, 31]; we still chose GRI3.0 for the present work because extinction strain rate computations are computationally intensive and time consuming. The comprehensive models contain a robust treatment of low-temperature chemistry (mainly for ignition delay calculations) that do not affect the extinction strain rate or flame speed predictions. This may however affect the plasma coupling, and different models will be examined in the future, when the plasma is incorporated in the calculations. The upper bound for our NO_x estimates are zerostrain flamelet models (modeled using the FreeFlame module in Cantera) and the lower bound are the flames at the largest residence times possible, i.e. flamelets at the extinction strain rate. NO_x values within these bounds are depicted as the shaded region in the figure. The highest emissions recorded experimentally in the data is nearly 25 ppm at stoichiometric conditions. For the leanest condition we could operate the combustor, i.e. at $\phi = 0.6$, the emissions were below the detection limit of 2 ppm. These results suggest that the emissions from the flame correspond to a flame that is effectively a strained flame. This should not imply that the strain-rates are the same at all points of the flame, but rather, despite different parts of the flame experiencing different strains, the combined emissions from all these flamelets, when added up are still within the bounds of a strained flamelet.

Figure 8 (left) also depicts the NO_x levels with the NRPD operated at conditions corresponding to 8.64 mJ/pulse at various equivalence ratios. This pulse energy is well above the minimum energy required to completely suppress combustion instabilities but leads to NO_x levels increasing to a constant level, independent of the equivalence ratio.

The effect of pulse energy on excess NO_x production due to the discharges is plotted in Figure 8 (right). The case of zero pulse energy corresponds to no plasma and the emissions are thus purely due to the flame. At pulse energies of 6 mJ/pulse, we begin to see instability reduction but not complete suppression. There is a larger parametric space to be explored by changing the pulse frequency, moving the electrode closer to the flame etc. and to observe if NO_x can be further reduced. As NO_x emissions seem to increase with per-pulse energy, optimizing the energy delivery of the plasma can help with the emissions problem (see section IIIC).

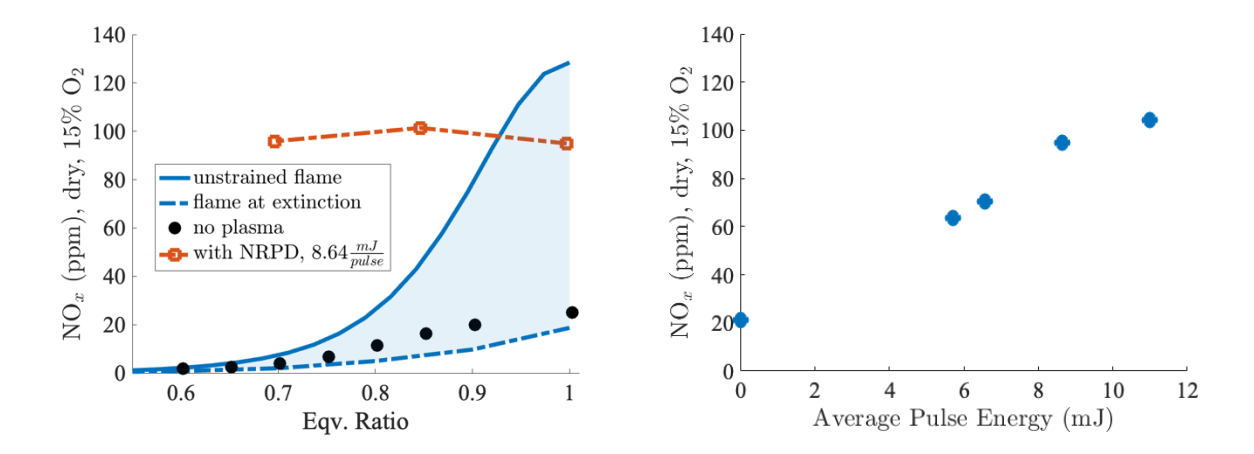


Figure 8: (Left) NO_x emissions from CH₄/air flames with and without plasma for different equivalence ratio and comparison with two flamelet models. Simulations are for the no-plasma case. (Right) Effect of NRPD pulse energy on NO_x emissions for a stoichiometric CH₄/air flame.

NO_x emissions were also measured for CH₄/NH₃ flames. However, there are two limitations at present in our setup. The first is the level of emissions for most operating conditions with NH₃ which far exceeds the 5000 ppm limit of our measurement system. The second is that beyond 80%/20% NH₃/CH₄ ratios, the flame wouldn't anchor. For these mixtures as the equivalence ratio is decreased, NO_x increases again beyond the limits of our emissions analysis system. Therefore we report just a single measurement set (with and without plasma) in Figure 9. Nevertheless, for this case we observe that the NRPD discharges reduce NO_x levels. Without plasma, we observed NO_x emissions of 2684 ppm, mainly NO. NO₂ in the total NO_x is less than 1%. With a nanosecond pulsed plasma at 9 kHz, the NO_x levels reduced to 2307 ppm, corresponding to a 10% reduction. For comparison, we also plot results from simulations of flamelet models in the same figure. These two limits are the bounds of the unstrained flame and strained flames at extinction as was explained in the context of Figure 8 (left). Unlike the case of methane/air flames, the NO_x measurements for CH₄/NH₃ flames are much less than those predicted by two kinetic models we studied. The model by Okafor et al. [32] is one of the earliest models used for CH₄/NH₃ flames that is built from the GRI 3.0 mechanism. The second is the most recent (2023-2024) CEU mechanism from KAUST which was validated against NO_x measurements in a counterflow-flame reactor [33, 34]. Interestingly, both mechanisms predict very similar burning velocities and extinction strain rates, but the NO_x emissions vary by more than 100% in some cases. Further work is needed to identify a suitable kinetic model, including plasma, that can match the experimental data to understand why the NRPD discharges reduce NO_x for CH₄/NH₃ flames.

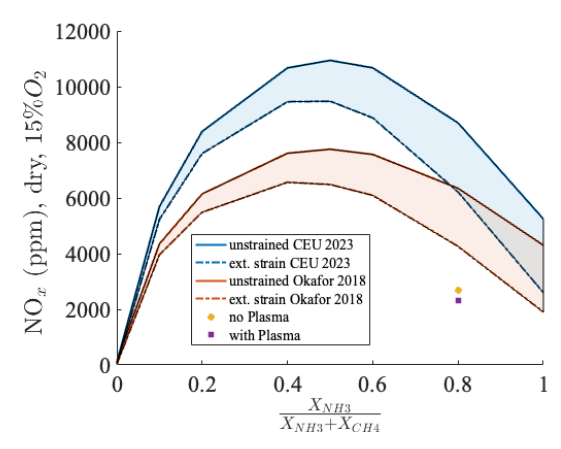


Figure 9: NO_x emissions from CH₄/NH₃/air flames with and without plasma and comparisons with two flamelet models. Calculations are for the no-plasma case.

IV. Conclusions

The objective of this work was to report preliminary results on flame macrostructures, combustion instability characteristics and NO_x emissions with and without nanosecond repetitively pulsed discharges for turbulent, swirling, CH₄/NH₃ flames in an atmospheric pressure burner. In this burner combustion dynamics were observed for a range of equivalence ratios at various frequencies and amplitudes; and the NRPD's successfully suppressed them for all conditions. Next we observed that the NPRD has a significant impact on the flame macrostructure that changes form a lifted compact flame (that is seen without plasma) to a compact and anchored flame due to the discharges. Even with ammonia flames, in this setup we observed compact macrostructures where we (and others in literature) previously observed longer flames. Finally, we measured NO_x emissions at NPRD power levels necessary to suppress combustion dynamics in these flames. With the NPRD, the NO_x increases depending on the discharge power levels, for pure methane; but reduces for flames with larger fractions of ammonia. We also attempted to model these emissions using flamelet models (no plasma case) and found that for pure methane flames, these emissions are bounded by predictions of flamelet at zero-strain and flamelets at the flames' extinction strain rate. For ammonia/methane blends however, more research seems necessary to develop kinetic models whose predictions match experimental data in burner flames.

Acknowledgments

This work was supported by the Department of Energy SBIR program, award number DE-SC1870000, the Office of Naval Research, award number N00014-21-1-2572, and the National Science Foundation, NSF, award number 2339518. We would like to thank Drew Weibel, Oliver Dyakov and Issac Kramer from Specter Aerospace for their assistance at various stages of the project.

References

- ¹ Miller, Cassandra J., Prakash Prashanth, Florian Allroggen, Carla Grobler, Jayant S. Sabnis, Raymond L. Speth, and Steven RH Barrett. "An environmental cost basis for regulating aviation NOx emissions." Environmental Research Communications 4, no. 5 (2022): 055002.
- ² Pugh, Daniel, Philip Bowen, Burak Goktepe, Anthony Giles, Syed Mashruk, Agustin Valera Medina, and Steven Morris. "Influence of Steam and Elevated Ambient Conditions on N2O in a Premixed Swirling NH3/H2 Flame." In Turbo Expo: Power for Land, Sea, and Air, vol. 86953, p. V03AT04A064. American Society of Mechanical Engineers, 2023.
- ³ Pugh, Daniel, Philip Bowen, Agustin Valera-Medina, Anthony Giles, Jon Runyon, and Richard Marsh. "Influence of steam addition and elevated ambient conditions on NOx reduction in a staged premixed swirling NH3/H2 flame." Proceedings of the combustion institute 37, no. 4 (2019): 5401-5409.
- ⁴ Wang, Shixing, Zhihua Wang, and William L. Roberts. "Measurements and simulations on effects of elevated pressure and strain rate on NOx emissions in laminar premixed NH3/CH4/air and NH3/H2/air flames." Fuel 357 (2024): 130036.

- ⁵ Wang, Guoqing, Thibault F. Guiberti, Santiago Cardona, Cristian Avila Jimenez, and William L. Roberts. "Effects of residence time on the NOx emissions of premixed ammonia-methane-air swirling flames at elevated pressure." Proceedings of the Combustion Institute 39, no. 4 (2023): 4277-4288.
- ⁶ Wang, Guoqing, Thibault Guiberti, and William Roberts. "Exploring the effects of swirl intensity on NO emission in ammonia-methane-air premixed swirling flames." Journal of Ammonia Energy 1, no. 1 (2023): 74-82.
- ⁷ Mashruk, Syed, Ali Alnasif, Chunkan Yu, James Thatcher, James Rudman, Lukasz Peronski, Chiong Meng-Choung, and Agustin Valera-Medina. "Combustion Characteristics of a Novel Ammonia Combustor equipped with Stratified Injection for Low Emissions." Journal of Ammonia Energy 1, no. 1 (2023): 21-32.
- ⁸ Cosway, Ben, Midhat Talibi, and Ramanarayanan Balachandran. "Investigation of NO production and flame structures in ammonia-hydrogen flames." Journal of Ammonia Energy 1, no. 1 (2023): 106-117.
- ⁹ Somarathne, K. D. K. A., Hatakeyama, S., Hayakawa, A., & Kobayashi, H. (2017). Numerical study of a low emission gas turbine like combustor for turbulent ammonia/air premixed swirl flames with a secondary air injection at high pressure. International Journal of Hydrogen Energy, 42(44), 27388-27399.
- ¹⁰ Gubbi, S., Cole, R., Emerson, B., Noble, D., Steele, R., Sun, W., & Lieuwen, T. (2024). Evaluation of Minimum NOx Emission From Ammonia Combustion. *Journal of Engineering for Gas Turbines and Power*, *146*(3).
- ¹¹ Gubbi, S., Cole, R., Emerson, B., Noble, D., Steele, R., Sun, W., & Lieuwen, T. (2023). Air Quality Implications of Using Ammonia as a Renewable Fuel: How Low Can NO x Emissions Go?. *ACS Energy Letters*, 8(10), 4421-4426.
- ¹² Choe, Jinhoon, Wenting Sun, Timothy Ombrello, and Campbell Carter. "Plasma assisted ammonia combustion: Simultaneous NOx reduction and flame enhancement." Combustion and Flame 228 (2021): 430-432.
- ¹³ Piumetti, Marco, Samir Bensaid, Debora Fino, and Nunzio Russo. "Catalysis in diesel engine NOx aftertreatment: a review." Catalysis, Structure & Reactivity 1, no. 4 (2015): 155-173.
- ¹⁴ Ju, Yiguang, and Wenting Sun. "Plasma assisted combustion: Dynamics and chemistry." Progress in Energy and Combustion Science 48 (2015): 21-83.
- ¹⁵ Anilkumar, A., Gajjar, P., & Bane, S. P. (2024). Influence of Nanosecond Repetitively Pulsed (NRP) Plasma Discharges on Atmospheric Pressure Premixed Swirl Stabilized Methane-Air Flames. In *AIAA SCITECH 2024 Forum* (p. 0599).
- ¹⁶ Kim, W., & Cohen, J. (2021). Plasma-assisted combustor dynamics control at realistic gas turbine conditions. *Combustion Science and Technology*, 193(5), 869-888.
- ¹⁷ Moeck, J., Lacoste, D., Laux, C., & Paschereit, C. (2013, January). Control of combustion dynamics in a swirl-stabilized combustor with nanosecond repetitively pulsed discharges. In 51st AIAA Aerospace Sciences Meeting including the New Horizons Forum and Aerospace Exposition (p. 565).
- ¹⁸ Lacoste, Deanna A. "Flames with plasmas." Proceedings of the Combustion Institute 39, no. 4 (2023): 5405-5428.
- ¹⁹ Dharmaputra, B., Shcherbanev, S., Schuermans, B., & Noiray, N. (2023). Thermoacoustic stabilization of a sequential combustor with ultra-low-power nanosecond repetitively pulsed discharges. *Combustion and Flame*, 258, 113101.
- ²⁰ Blanchard, Victorien P., Frédéric Roqué, Philippe Scouflaire, Christophe O. Laux, and Sébastien Ducruix. "Lean Flame Stabilization With Nanosecond Plasma Discharges in a Gas Turbine Model Combustor." In Turbo Expo: Power for Land, Sea, and Air, vol. 86953, p. V03AT04A074. American Society of Mechanical Engineers, 2023.
- ²¹ Kim, G. T., Park, J., Chung, S. H., & Yoo, C. S. (2024). Synergistic effect of non-thermal plasma and CH4 addition on turbulent NH3/air premixed flames in a swirl combustor. *International Journal of Hydrogen Energy*, 49, 521-532.
- ²² Tang, Y., Xie, D., Shi, B., Wang, N., & Li, S. (2022). Flammability enhancement of swirling ammonia/air combustion using AC powered gliding arc discharges. *Fuel*, *313*, 122674.
- ²³ Shanbhogue, Santosh J., Colin A. Pavan, Drew E. Weibel, Felipe Gomez del Campo, Carmen Guerra-Garcia, and Ahmed F. Ghoniem. "Control of Large-Amplitude Combustion Oscillations Using Nanosecond Repetitively Pulsed Plasmas." *Journal of Propulsion and Power* (2023): 1-13.
- ²⁴ Pavan, C. A., Shanbhogue, S. J., Weibel, D. E., del Campo, F. G., Ghoniem, A. F., & Guerra-Garcia, C. "Dynamic response of nanosecond repetitively pulsed discharges to combustion dynamics: regime transitions driven by flame oscillations" *Plasma Sources Science and Technology*, 33(2), 025016. (2024)
- ²⁵ Minesi, N. Q., V. P. Blanchard, Erwan Pannier, Gabi Daniel Stancu, and Christophe O. Laux. "Plasma-assisted combustion with nanosecond discharges. I: Discharge effects characterization in the burnt gases of a lean flame." *Plasma Sources Science and Technology* 31, no. 4 (2022): 045029.
- ²⁶ Shanbhogue, S., Abd El-Rahman, A., Boushaki, T., & Ghoniem, A. F. (2023). Dynamic Stability Characteristics of CH4/NH3 Mixtures. In *AIAA AVIATION 2023 Forum* (p. 3805).

- ²⁷ Khateeb, A. A., Guiberti, T. F., Zhu, X., Younes, M., Jamal, A., & Roberts, W. L. (2020). Stability limits and exhaust NO performances of ammonia-methane-air swirl flames. *Experimental Thermal and Fluid Science*, 114, 110058.
- ²⁸ Zhang, M., An, Z., Wang, L., Wei, X., Jianayihan, B., Wang, J., ... & Tan, H. (2021). The regulation effect of methane and hydrogen on the emission characteristics of ammonia/air combustion in a model combustor. *International Journal of Hydrogen Energy*, 46(40), 21013-21025.
- ²⁹ Guerra-Garcia, C., & Pavan, C. A. (2023). The backward problem in plasma-assisted combustion: Experiments of nanosecond pulsed discharges driven by flames. *Applications in Energy and Combustion Science*, *15*, 100155.
- ³⁰ Sahu, A. B., Mohamed, A. A. E. S., Panigrahy, S., Saggese, C., Patel, V., Bourque, G., ... & Curran, H. J. (2022). An experimental and kinetic modeling study of NOx sensitization on methane autoignition and oxidation. *Combustion and Flame*, 238, 111746.
- ³¹ Panigrahy, S., Mohamed, A. A. E. S., Wang, P., Bourque, G., & Curran, H. J. (2023). When hydrogen is slower than methane to ignite. *Proceedings of the Combustion Institute*, *39*(1), 253-263.
- ³² Okafor, E. C., Naito, Y., Colson, S., Ichikawa, A., Kudo, T., Hayakawa, A., & Kobayashi, H. (2018). Experimental and numerical study of the laminar burning velocity of CH4–NH3–air premixed flames. *Combustion and flame*, 187, 185-198.
- ³³ Wang, S., Wang, Z., Chen, C., Elbaz, A. M., Sun, Z., & Roberts, W. L. (2022). Applying heat flux method to laminar burning velocity measurements of NH3/CH4/air at elevated pressures and kinetic modeling study. *Combustion and Flame*, *236*, 111788.
- ³⁴ Wang, S., Wang, Z., & Roberts, W. L. (2024). Measurements and simulations on effects of elevated pressure and strain rate on NOx emissions in laminar premixed NH3/CH4/air and NH3/H2/air flames. *Fuel*, 357, 130036.